Molecular dynamics simulations of PNA–PNA and PNA–DNA duplexes by the use of new parameters implemented in the GROMACS package: A conformational and dynamics study

ARTICLE *in* PHYSICAL CHEMISTRY CHEMICAL PHYSICS · DECEMBER 2013

Impact Factor: 4.49 · DOI: 10.1039/c3cp54284j · Source: PubMed

3 AUTHORS, INCLUDING:

Ida Autiero
Italian National Research Council
14 PUBLICATIONS **88** CITATIONS
SEE PROFILE

Michele Saviano
Italian National Research Council
248 PUBLICATIONS **3,007** CITATIONS
SEE PROFILE

PCCP

PAPER

Molecular dynamics simulations of PNA–PNA and PNA–DNA duplexes by the use of new parameters implemented in the GROMACS package: a conformational and dynamics study

Cite this: *Phys. Chem. Chem. Phys.*, 2014, **16**, 1868

Ida Autiero,[a] Michele Saviano*[b] and Emma Langella*[a]

Received 10th October 2013,
Accepted 15th November 2013

DOI: 10.1039/c3cp54284j

www.rsc.org/pccp

Peptide Nucleic Acids (PNAs) still represent a growing research area thanks to their potential applications in many fields of science from chemistry and biology to medicine. In these years, structural investigations by means of either experimental or computational techniques have proved to be very useful for the understanding of the structural organization and the binding properties of PNA. In this context, we here report an all-atoms Molecular Dynamics (MD) study of a PNA–PNA duplex and a PNA–DNA hetero-duplex with the well known GROMACS simulation package, by using new force field parameters properly derived for PNA molecules. The good agreement of our results with the crystallographic and NMR data, available for both the systems under investigation, confirms the validity of our approach. Moreover, our simulations reveal new interesting features related to the conformational-dynamic behavior of the studied systems, thus demonstrating the ability of MD simulations to gain insights into the dynamic properties of biologically relevant systems. This force field parametrization represents a good starting point for the implementation of a computational platform, based on the GROMACS package, useful for the rational design of modified PNA molecules with improved conformational features for selective binding toward DNA or RNA.

Introduction

Peptide nucleic acids (PNAs) are non-natural nucleic acid analogues[1,2] in which the phosphoribose backbone of DNA has been substituted with a pseudopeptide consisting of *N*-(2-aminoethyl)-glycine units with a methylene carbonyl linker connecting to the nucleobase (see Fig. 1). The charge-neutral backbone allows PNA to hybridize with the DNA or the RNA strand with high affinity,[3] while the unnatural polyamide linkage enables PNA to evade recognition and degradation by proteases and nucleases.[4] Moreover, PNA is much more mismatch sensitive than DNA, enabling sensitive and selective mismatch discrimination.

The simplicity of its structure with distinguishable properties, ease of synthesis and low toxicity have made PNA attractive as a putative genetic regulatory agent in antisense[5–7] and antigen[8–10] therapies. Promising applications of PNAs have appeared also in the emerging field of miRNAs which are non-coding RNAs having a significant role in gene regulation.[11]

Great efforts have been made in these years in order to improve PNA solubility, cellular uptake and binding specificity through the design of PNAs having different chemical modifications either in the backbone or in the nucleobases.[12–15] Moreover, useful insights into the structural features of both PNA–PNA duplexes and PNA–DNA/RNA hybrid duplexes or triplexes have been obtained by means of NMR[16–19] and X-ray crystallography.[20–29] These studies showed that PNA prefers a P-form helix, which is different from both the A- and B-forms of

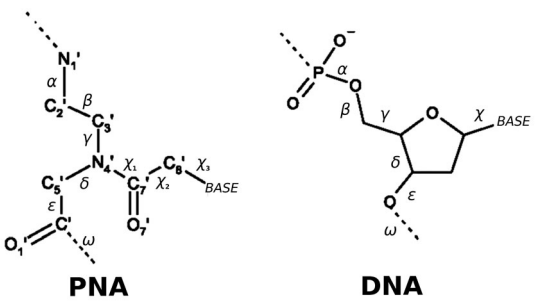

PNA-PNA *C-ter* Gpn-Gpn-Cpn-Apn-Tpn-Gpn-Cpn-Cpn *N-ter*
N-ter Cpn-Cpn-Gpn-Tpn-Apn-Cpn-Gpn-Gpn *C-ter*

PNA-DNA *C-ter* Gpn-Tpn-Apn-Gpn-Adl-Tdl-Cdl-Apn-Cpn-Tpn *N-ter*
3' C - A - T - C -T -A - G - T - G - A *5'*

Fig. 1 Top: chemical structure of PNA (left) and DNA (right) oligomers. Down: PNA–PNA (18) and PNA–DNA (42) duplex sequences.

[a] *National Research Council, Institute of Biostructures and Bioimaging, 80138 Naples, Italy. E-mail: emma.langella@cnr.it*
[b] *National Research Council, Institute of Crystallography, 70126 Bari, Italy. E-mail: msaviano@unina.it*

RNA and DNA, being more unwound and having a larger diameter than DNA duplexes.

Very recently, interesting results concerning the effect of specific chemical modifications on the structural preferences of PNA have been obtained not only by experimental structural techniques,[20,21,29] but also through computational studies.[30–33] Indeed, both experimental[16–29] and computational studies[30–40] have proven to be useful for the understanding of the structural organization and the binding properties of PNA, and for the development of more effective modified PNAs for targeting DNA and RNA. However, very few works on the use of MD for PNA structural analysis have so far been reported.[30–40] Indeed, the fact that PNAs are non-standard residues makes MD studies a more challenging task, because PNA residues need to be accurately parametrized into the force field prior to performing simulations.

In this scenario, we have derived new force field parameters to mimic the PNA behavior in the GROMACS simulation package.[41] Reliability of parametrization has been tested by performing all-atoms Molecular Dynamics simulations on two case systems, a PNA–PNA (hereafter PP) duplex and a PNA–DNA (hereafter PD) hetero-duplex (Fig. 1). The above systems have been chosen as case studies, because their structures have been determined experimentally and are available for a comparison with simulations results.[18,29] The PP duplex is a palindromic 8-base pair duplex for which both NMR[18] and X-ray structures[20] are available (Fig. 1). The PD duplex is an antiparallel 10-base pair duplex, containing three adjacent chiral monomers based on D-Lys in the middle of the PNA sequence,[42] and its structure has been determined by means of X-ray diffraction (Fig. 1).[29] Helical parameters and dihedral angles, together with other general trends, have been carefully evaluated on both test-systems in order to assess the accuracy of the parametrization.

Interesting conformational features, not detected in previous structural investigations, are revealed from our results. To the best of our knowledge this is the first time that the parametrization of PNA-like molecules is carried out in GROMACS.

The force field parametrization underlying this study will allow further studies of other homo- or hetero-duplexes as well as triplexes containing PNA molecules, with useful applications in different fields of biomedical interest.

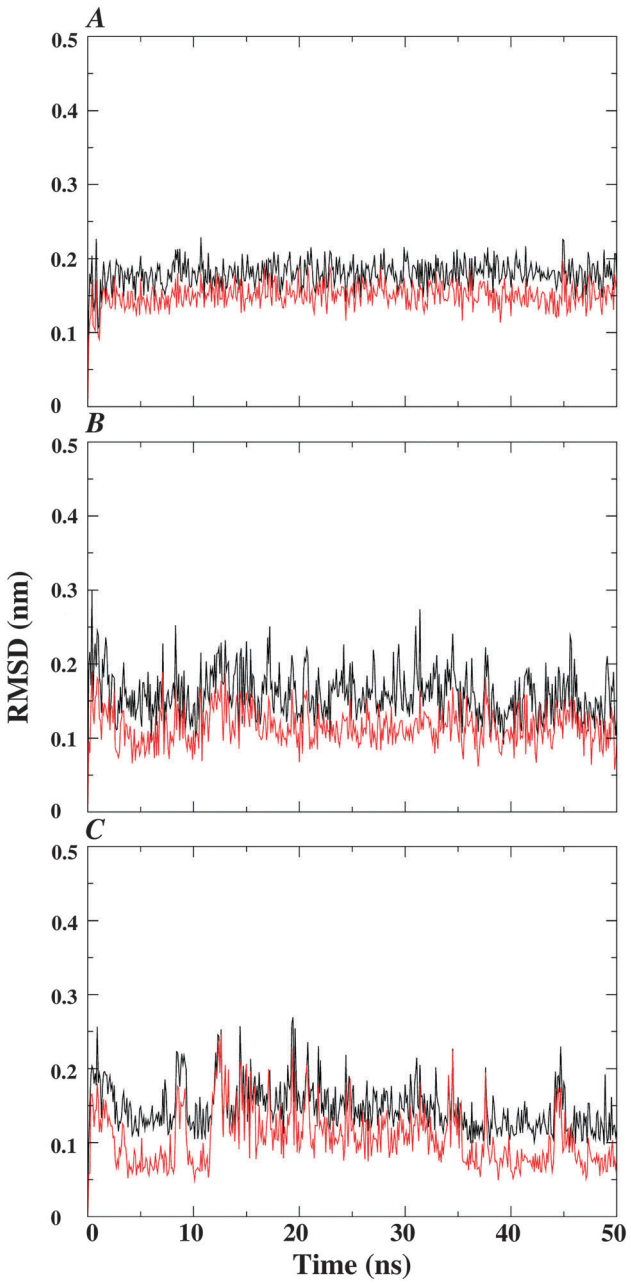

Fig. 2 Root Mean Square Deviation (RMSD) calculated for the backbone (black) and the nucleobase atoms (red). PNA–PNA duplex (A). PNA–DNA duplex: DNA strand (B) and PNA strand (C).

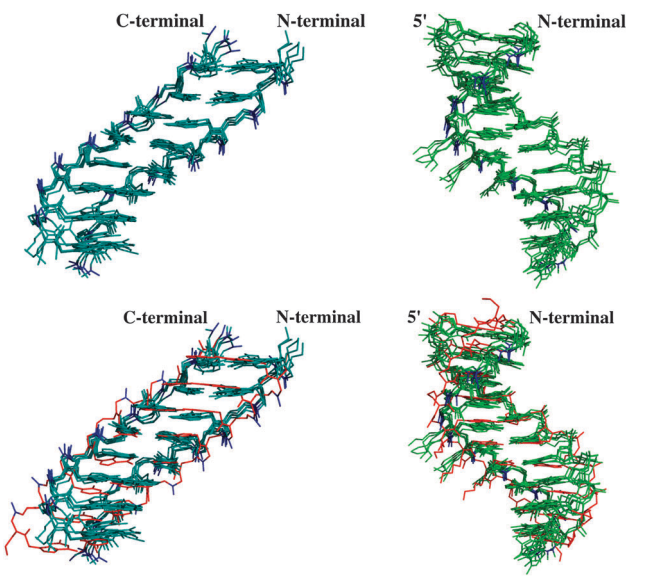

Fig. 3 Top: superimposition of 5 MD derived structures of the PNA–PNA duplex (left/cyan) and the PNA–DNA duplex (right/green). The atoms are displayed in sticks and carbonyl groups are in blue. Down: superimposition of 5 MD derived structures of the PNA–PNA duplex (left/cyan) with the NMR structure (red) and the PNA–DNA duplex (right/green) with the crystallographic structure (red). The atoms are displayed in sticks and carbonyl groups are in blue.

Method

The structures of the PP and PD duplexes were downloaded from the Protein data bank database, using the NMR (PDB id: 1NR8)[18] and crystallographic (PDB id: 2K4G)[29] structures, respectively. For the PP duplex, the minimized average structure was extracted from the NMR ensemble as our starting model for the molecular dynamics simulation. In the case of PD, only the DNA and PNA coordinates were considered, so both the structures were modified by removing terminal capping groups, ions and water molecules from the coordinate file.

Molecular dynamics (MD) simulations were performed and analysed using the GROMACS simulation package.[41] The Parmbsc0[43] force field, a refinement of the AMBER parm99[44] force field for nucleic acids, was employed for the simulations. Since the PNA residues are not recognized by the force field,

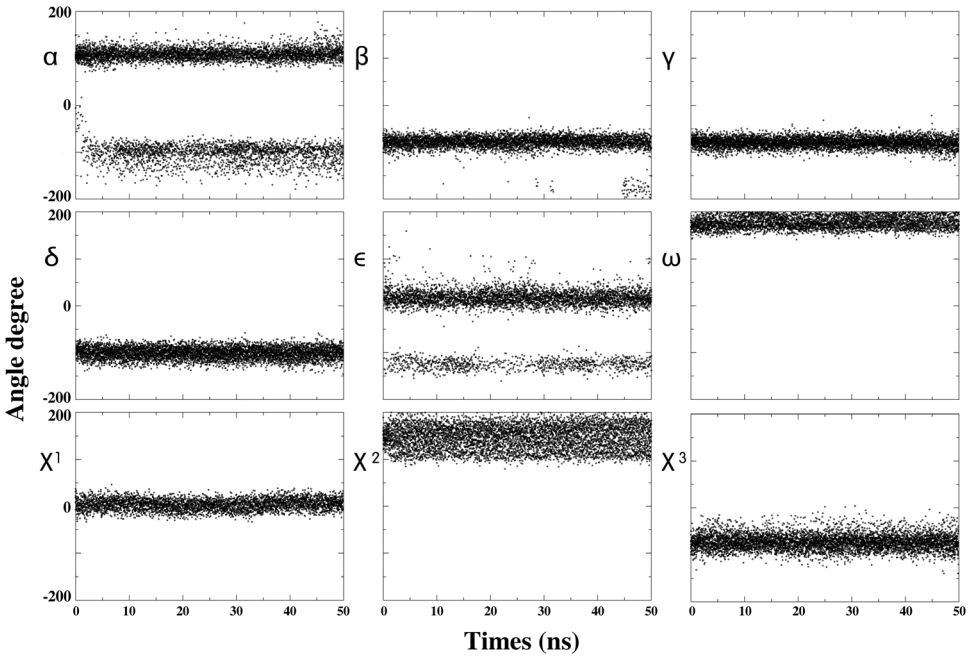

Fig. 4 Variation of the PNA strand torsional angles along the PNA–PNA molecular dynamics simulation.

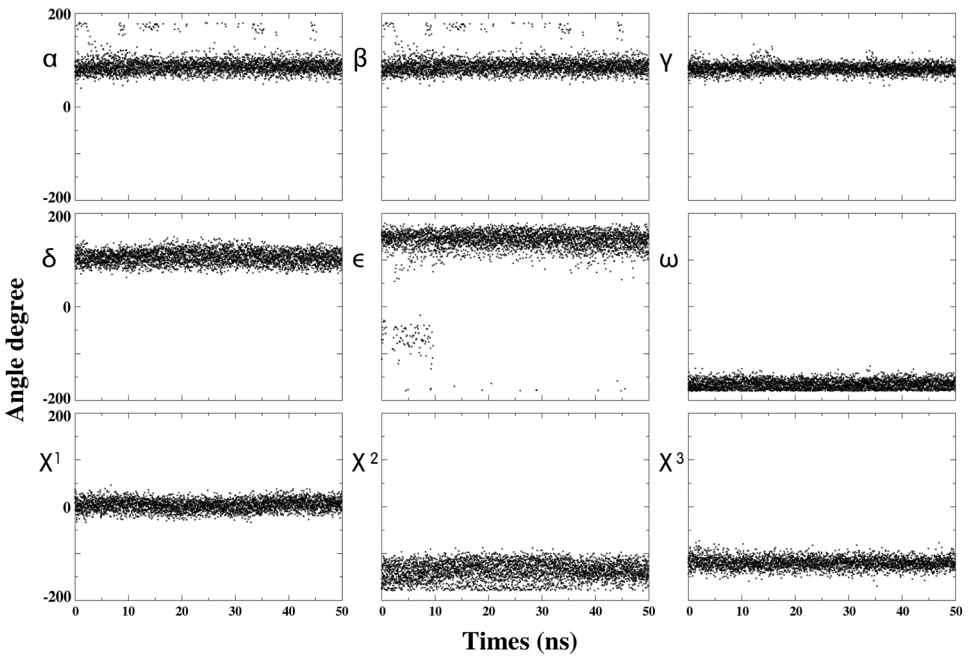

Fig. 5 Variation of the PNA strand torsional angles along the PNA–DNA molecular dynamics simulation.

these parameters were manually assigned. To do this, bonded and van der Waals parameters were assigned taking into account the corresponding values in standard peptidic and nucleobase fragments, included in the Amber99sb force field library. The atomic charges of the peptide and nucleobase portions, of each PNA residues, were separately obtained by the use of the RESP ESP charge Derive (R.E.D.) Server[45] and following the protocol used by Cornell *et al.*[46] In detail, the truncated bonds of each fragments were capped with conventional moieties. The geometries of the crystal were preserved, while the capping fragments were geometrically optimized (at the semi-empirical level), and, finally, all the partial charges were derived by quantum mechanical calculations (HF/6-31G*) using Gaussian 09, as implemented in the R.E.D. Server.

Then, the models were solvated in an octahedron box filled of TIP3P water molecules with at least a 9 Å distance to the border adding counter-ions to neutralize the system. The simulations were run under NPT conditions (300 K and $P = 1$ bar) with Berendsen' coupling algorithm.[47] Periodic boundary conditions were employed and the LINCS algorithm[48] was used to constrain all bond lengths. An integration time step of 2 fs was used. The particle mesh Ewald method was applied to treat electrostatic interactions,[49,50] and a nonbonded cutoff of 1.4 nm was used for the Lennard-Jones potential. In both systems, the water molecules were relaxed by energy minimization and followed by 10 ps of MD at 300 K, restraining the PNA and DNA atomic positions with a harmonic potential. Then, both PP and PD systems were heated up gradually to 300 K in a five step process, starting from 50 K to 300 K. After this step, the systems were simulated under NPT standard conditions for 50 ns without restraints. The analysis of the MD trajectories was done by the use of the GROMACS package and the Curves program[51] for the calculation of helical parameters.

Results and discussion

Overall system stability throughout the simulations

Over the duration of the simulations, both the duplexes maintain stable helical structures with well-defined base pairing and base stacking. Root-mean-square deviation (RMSD) values have been calculated and reported in Fig. 2 for the duplex backbones as well as for the nucleobases. Analysis of RMSDs clearly reveals that the systems rapidly reach equilibrium and are stable during the whole simulation time. Moreover, the base RMSDs were consistently smaller than those of the PNA backbone. In fact, despite the higher PNA backbone flexibility, nucleobases occupy stable positions, thus indicating an important role for base stacking in the stabilization of PNA duplexes, in agreement with previous studies.[17,18,29,38,40]

In the case of the PD duplex, the global system stability is also mirrored by the RMSD values computed for the DNA strand during the simulation (Fig. 2). The analysis of the RMSD trends for the PNA and the DNA strands reveals a comparable behavior, thus suggesting that both the strands tend to adapt to the newly formed double-helix, as already hypothesized in previous works.[20,24,29,38]

Table 1 Dihedral angles of PNA strands in PP and PD duplexes. Average values (degrees) computed throughout the simulation and the corresponding standard deviations (in parentheses) are reported. Experimental values are reported for comparison

	α	β	γ	δ	ε	ω	χ^1	χ^2	χ^3
PNA–PNA (this work)	108.7 (12) −103.3 (19.9)	−81.3 (20.2)	−79.6 (10.7)	−101 (12.5)	−124.6 (10.9) 17.6 (15.7)	180.4 (15.2)	0.04 (11.5)	146.9 (26)	−73.1 (16.8)
PNA—PNA[18]	−93 (24) 123 (16)	−66 (5)	−75 (4)	−88 (10)	−155 (17) −3 (12)	175 (10)	2 (4)	169 (10)	−82 (8)
PNA–PNA[20]	−123.1 (10.6) 76.15 (3.6)	65.6 (8.3)	70.5 (7.1)	83.0 (8.4)	8.1 (5.1) −165 (11.4)	173.3 (5.7)	8.2 (2.6)	−177.1 (1.3)	81.8 (6.0)
DNA–PNA (this work)	103 (17) −106 (13.2)	88 (17.6)	82.1 (9.5)	106.2 (14)	143.57 (16.9) −82.1 (42.5)	−167 (9.6)	3.8 (12)	−136.1 (18.2)	−120.4 (11.7)
DNA–PNA[29]	−114 (15) 72 (7)	73 (9)	67 (4)	90 (5)	179 (10) −21	−178 (2)	4 (6)	−178 (3)	−91 (6)

Fig. 3 shows a superposition of 5 MD derived structures (extrapolated every 10 ns of simulation) of both PP and PD duplexes with the corresponding experimental structures. As expected on the basis of RMSD plots, the structural similarity between these structures is higher in the base pair region than in the backbone region, and it is also higher in the central part of the duplex than at the end of the duplex.

Inspection of Fig. 3 (upper panel) also reveals that MD structures are able to well represent the carbonyl group conformation of the linker that connects the nucleobase to the backbone, which is oriented towards the C-end of the PNA strands in both PP and PD systems, in agreement with the experimental structures. This orientation has also been reported in previous PNA structures,[17,18,20,24,29] and generates a significant helix dipole as can be seen in Fig. 3.

Conformational variability: PNA torsion angles

Backbone (α–ω), as well as linker (χ^1–χ^3) PNA torsion angles (Fig. 1) have been measured throughout the simulation (Fig. 4 and 5) for both PP and PD duplexes. Average values are listed in Table 1, together with the corresponding values in the experimental structures. In the case of the PP duplex, both the available NMR[18] and crystallographic data[20] have been reported. All the analyses were performed over the central 6 and 8 residues for the PP and PD duplexes, respectively. These data reveal that all the dihedral values are consistent with those reported for the NMR and X-ray structures of PP and PD systems, respectively. In detail, no transitions are observed, thus indicating stable trajectories, rather, dihedrals slightly fluctuate around an average value. The only exception is represented by α and ε angles, which can assume two values, as shown in Table 1 and Fig. 4 and 5, in agreement with previous studies.[18,37,38,40] These angles are correlated with each other and with the orientation of the backbone amide group. Moreover, in both the duplexes, α and ε show high amplitude of fluctuations with respect to the other angles, in agreement with experimental data, which indicates large flexibility of the PNA backbone, especially in the α and ε bonds.[16,17,38,40]

In both PP and PD, the planarity of the amide bonds in the backbone is well-maintained, as reflected by the *ca.*180° and 0° values of the ω and χ^1 angles, respectively.

Concerning the PNA linkers, χ^1 and χ^3 torsions are narrowly distributed, whereas χ^2 shows large amplitude motions in both PP and PD duplexes. However, this flexibility does not affect either Watson–Crick base pairing or base stacking, which are relevant for PNA duplex stability. This particular behavior of the χ^2 torsion angle, which has never been discussed in previous experimental investigations, could explain the ability of the PNA to adopt different conformations avoiding dramatic changes in the position of the nucleobases.

Helical parameters

For the simulated systems helical parameters have been computed and compared with those of the corresponding experimental structures, using the Curves program.[51] Obtained parameters are listed in Table 2. For comparison, A-DNA and B-DNA helical parameters are also reported in Table 2.

It is worth noting that parameters, obtained for both the PP and the PD helices, are in good agreement with those reported for the NMR and the crystallographic structures, respectively. From a more general point of view, the helical parameters computed for the simulated PNA–PNA duplex are typical of P-like helices. P-helix, which is the preferred conformation of PNA duplexes[24] is characterized by large base pair displacement from the helical axis and small twist angles. Consequently, PNA duplexes are wider and more unwounded than B-DNA duplexes, with a number of base pairs per helical turn larger than that in either DNA or RNA (10–12 bp per turn). Structures obtained from our MD trajectories comply with those features (see Table 2).

In particular, *x*-displacement values of 4.5 Å and 3 Å and twist values of 16.6° and 27.9° were obtained for PP and PD duplexes, respectively. Moreover, other helical parameters, like ''rise'' and ''tilt'', are also in good quantitative agreement with the experimental counterparts in both PP and PD systems.

It is interesting to note that, in the PD system, the twist angle (27.9°) slightly deviates from the crystallographic one (23.2°), leading to a lower value of bases per turn. Even though helical values fall globally into the range of a P-like helix conformation, such differences in term of twist values with the X-ray structure are putatively addressed to crystal-packing effects. This hypothesis is further supported by the good quantitative agreement with data obtained for a different PD duplex by NMR spectroscopy,[19] where packing effects are missing and the system is free to move into the solvent, as for MD simulations. On the other hand, a significant degree of variability in the average twist angles of other PNA–DNA duplexes has been previously reported in other MD studies.[30–40] Thus, our simulations are able to capture some dynamical aspects, which can be important for the full understanding of the conformational

Table 2 Helical parameters of PP and PD duplexes. Average values were computed on 5 representative structures of each system using the Curves program (ref. 51). Experimental values are reported for comparison

	x-Disp (Å)	Rise (Å)	Tilt (°)	Twist (°)	bp
PNA–PNA (this work)	4.5 (3.3)	3.2 (0.1)	−0.2 (0.8)	−16.6 (1)	21.7
PNA–PNA[18]	7.9	3.7	−0.2	−17.3	21
PNA–PNA[20]	8.4	3.2	−0.3	−18.8	19
PNA–DNA (this work)	−3 (0.4)	3.3 (0.1)	−1.7 (1.1)	27.9 (0.8)	13
PNA–DNA[29]	−3.8	3.5	−1.1	23.2	15.5
PNA–DNA[19]	3.8	3.3	—	28	13
A-DNA[52]	−4.5	2.6	−4.5	32.7	11
B-DNA[52]	0	3.4	−0.1	36	10

behavior of the system, complementing the experimental crystallographic data.

Finally, in agreement with NMR and crystallographic structures both the PP and PD duplexes show a narrower minor groove with respect to that of the B-DNA duplexes, likely due to the neutral PNA backbone.

Conclusions

MD simulations of a palindromic PNA–PNA duplex and of a PNA–DNA hetero-duplex have been carried out with the GROMACS simulation package (Fig. 1), by using new force field parameters accurately derived for PNA residues. In order to assess the validity of the underlying parametrization, the results obtained from our simulations have been compared with the experimental structures[18,20,29] available for both the systems.

Data analysis shows that reliable results have been obtained for both test-systems. In detail, the computed helical parameters as well as all the dihedral angles are in good quantitative agreement with experimental counterparts. Moreover, our simulations are able to well reproduce detailed structural features of the two studied systems, as the orientation of the carboxylic bond of the linker region, as well as the two-ranges of values assumed by α and ε dihedral angles.

Interestingly, our analysis allows us to put forward new conformational features, not detected by previous structural investigations, which are related to dynamics of the systems, such as the flexibility of the linker region (related to the χ^2 angle), for both the PP and PD systems, and the small deviation of the helical twist in the PD duplex. In the latter case, during our simulations, the helical twist was driven to a value definitely closer to the NMR-like helix conformation,[19] getting over the crystal-packing effect present in the original X-ray structure, in line with the expectation that NMR and MD techniques are able to describe the dynamics of the system.

In summary, we have demonstrated that molecular dynamics simulations are able to correctly describe the behavior of interesting biological systems, as the PNA, when proper force field parameters are assigned. Moreover, reliability of our simulations allows their use also to predict the conformational properties of other homo- or hetero-duplexes as well as triplexes containing DNA molecules, and demonstrates that this technique is a valid complement to the experimental observations. In addition, to our knowledge, this is the first time that a parametrization procedure for PNA residues is carried out in GROMACS.[41] GROMACS is a fast and versatile simulation package, widely used by the scientific community for performing MD simulations, thus it is of interest to make it applicable to a broader set of general interest molecules.

In conclusion, the present work represents a good starting point for the implementation of a computational platform, useful for the rational design of modified PNA molecules, with improved conformational features, for selective binding toward DNA and/or RNA.

Acknowledgements

The authors would like to give their special thanks to Mr Luca de Luca, Dr Lucrezia Cassano and Dr Caterina Chiarella for technical assistance. This work was supported by the Fondazione CON IL SUD (2011-PDR-20).

References

1 P. E. Nielsen, M. Egholm, R. H. Berg and O. Buchardt, *Science*, 1991, **254**, 1497–1500.
2 P. E. Nielsen and M. Egholm, *Peptide Nucleic Acids*, Horizon Scientific Press, Wymondham, UK, 1999.
3 K. K. Jensen, H. Orum, H. P. E. Nielsen and B. Norden, *Biochemistry*, 1997, **36**, 5072–5077.
4 V. V. Demidov, V. N. Potaman, M. D. Frank-Kamenetskii, M. Egholm, O. Buchard, S. H. Sonnichsen and P. E. Nielsen, *Biochem. Pharmacol.*, 1994, **48**, 1310–1313.
5 P. E. Nielsen, *Curr. Opin. Struct. Biol.*, 1999, **9**, 353.
6 U. Koppelhus and P. E. Nielsen, *Antisense Drug Technology*, ed. S. T. Crooke, Marcel Dekker Inc., New York, 2001, 359.
7 J. C. Hanvey and L. E. Babiss, in *Delivery Strategies for Antisense Oligonucleotide Therapeutics*, ed. S. Akhtar, CRC Press Inc., Boca Raton, Editon edn 1995, 151.
8 R. Gambari, *Curr. Top. Pharmacol.*, 2004, **8**, 313.
9 S. Cogoi, A. Codognotto, V. Rapozzi and L. E. Xodo, *Nucleosides Nucleotides Nucleic Acids*, 2005, **24**, 971–974.
10 V. L. Marin, S. Roy and B. A. Armitage, *Expert Opin. Biol. Ther.*, 2004, **4**, 337–348.
11 Z. Liu, A. Sall and D. Yang, *Int. J. Mol. Sci.*, 2008, **9**, 978–999.
12 K. N. Ganesh and V. A. Kumar, *Acc. Chem. Res.*, 2005, **38**, 404–412.
13 K. N. Ganesh and V. A. Kumar, *Curr. Top. Med. Chem.*, 2007, **7**, 715–726.
14 P. E. Nielsen, *Acc. Chem. Res.*, 1999, **32**, 624–630.
15 P. E. Nielsen and K. N. Ganesh, *Curr. Org. Chem.*, 2000, **4**, 931–943.
16 S. C. Brown, S. A. Thomson, J. M. Veal and D. G. Davis, *Science*, 1994, **265**, 777–780.
17 C. M. Topham and J. C. Smith, *J. Mol. Biol.*, 1999, **292**, 1017–1038.
18 W. He, E. Hatcher, A. Balaeff, D. N. Beratan, R. R. Gil, M. Madrid and C. Achim, *J. Am. Chem. Soc.*, 2008, **130**, 13264–13273.
19 M. Eriksson and P. E. Nielsen, *Nat. Struct. Biol.*, 1996, **3**, 410–413.
20 J. I. Yeh, E. Pohl, D. Truan, W. He, G. M. Sheldrick, S. Du and C. Achim, *Chemistry*, 2010, **16**, 11867–11875.
21 J. I. Yeh, B. Shivachev, S. Rapireddy, M. J. Crawford, R. R. Gil, S. Du, M. Madrid and D. H. Ly, *J. Am. Chem. Soc.*, 2010, **132**, 10717–10727.
22 B. Petersson, B. B. Nielsen, H. Rasmussen, I. K. Larsen, M. Gajhede, P. E. Nielsen and J. S. Kastrup, *J. Am. Chem. Soc.*, 2005, **127**, 1424–1430.
23 H. Rasmussen, T. Liljefors, B. Petersson, P. E. Nielsen and J. S. Kastrup, *J. Biomol. Struct. Dyn.*, 2004, **21**, 495–502.

24 B. Petersson, B. B. Nielsen, H. Rasmussen, I. K. Larsen, M. Gajhede, P. E. Nielsen and J. S. Kastrup, *Proc. Natl. Acad. Sci. U. S. A.*, 2003, **100**, 12021–12026.

25 B. Eldrup, B. B. Nielsen, G. Haaima, H. Rasmussen, J. S. Kastrup, C. Christensen and P. E. Nielsen, *Eur. J. Org. Chem.*, 2001, 1781–1790.

26 G. Haaima, H. Rasmussen, G. Schmidt, D. K. Jensen, J. S. Kastrup, P. W. Stafshede, B. Norden, O. Buchardt and P. E. Nielsen, *New J. Chem.*, 1999, **23**, 833–840.

27 H. Rasmussen, J. S. Kastrup, J. N. Nielsen, J. M. Nielsen and P. E. Nielsen, *Nat. Struct. Biol.*, 1997, **4**, 98–101.

28 L. Betts, J. A. Josey, J. M. Veal and S. R. Jordan, *Science*, 1995, **270**, 1838–1841.

29 V. Menchise, G. De Simone, T. Tedeschi, R. Corradini, S. Sforza, R. Marchelli, D. Capasso, M. Saviano and C. Pedone, *Proc. Natl. Acad. Sci. U. S. A.*, 2003, **100**, 12021–12026.

30 S. K. Gupta, S. Sur, O. R. Prasad and V. Tandon, *Mol. Biosyst.*, 2013, **9**, 1958–1971.

31 S. Sharmaa, B. S. Uddhavesh and R. J. Rajendra, *J. Biomol. Struct. Dyn.*, 2010, **27**, 663–676.

32 K. Siriwong, P. Chuichay, S. Saen-oon, C. Suparpprom, T. Vilaivan and S. Hannongbua, *Biochem. Biophys. Res. Commun.*, 2008, **372**, 765–771.

33 J. A. Ortega, J. R. Blas, M. Orozco, A. Grandas, E. Pedroso and L. Robles, *J. Org. Lett.*, 2007, **9**, 4503–4506.

34 J. Panecka, C. Mura and J. Trylska, *J. Phys. Chem. B*, 2011, **115**, 532–546.

35 P. Weronski, Y. Jiang and S. Rasmussen, *Biophys. J.*, 2007, **92**, 3081–3091.

36 I. Dilek, M. Madrid, R. Singh, C. P. Urrea and B. A. Armitage, *J. Am. Chem. Soc.*, 2005, **127**, 3339–3345.

37 T. Rathinavelan and N. Yathindra, *FEBS J.*, 2005, **16**, 4055–4070.

38 R. Soliva, E. Sherer, F. J. Luque, C. A. Laughton and M. Orozco, *J. Am. Chem. Soc.*, 2000, **122**, 5997–6008.

39 G. C. Shields, C. A. Lauthton and M. Orozco, *J. Am. Chem. Soc.*, 1998, **120**, 5895S–5904S.

40 S. Sen and L. Nilsson, *J. Am. Chem. Soc.*, 1998, **120**, 619–631.

41 D. van der Spoel, E. Lindahl, B. Hess, G. Groenhof, A. E. Mark and H. J. C. Berendsen, *J. Comput. Chem.*, 2005, **26**, 1701–1718.

42 S. Sforza, R. Corradini, S. Ghirardi, A. Dossena and R. Marchelli, *Eur. J. Org. Chem.*, 2000, 2905–2913.

43 V. Hornak, R. Abel, A. Okur, B. Strockbine, A. Roitberg and C. Simmerling, *Proteins*, 2006, **65**, 712–725.

44 A. Pérez, I. Marchán, D. Svozil, J. Sponer, T. E. Cheatham, C. A. Laughton and M. Orozco, *Biophys. J.*, 2007, **92**, 3817–3829.

45 E. Vanquelef, S. Simon, G. Marquant, E. Garcia, G. Klimerak, J. C. Delepine, P. Cieplak and F. Y. Dupradeau, *Nucleic Acids Res.*, 2011, **39**(web server issue), W511–W517.

46 W. D. Cornell, P. Cieplak, C. I. Bayly, I. R. Gould, K. M. Merz, D. M. Ferguson, D. C. Spellmeyer, T. Fox, J. W. Caldwell and P. A. Kollman, *J. Am. Chem. Soc.*, 1995, **117**, 5179–5197.

47 H. J. C. Berendsen, J. P. M. Postma, W. F. Van Gunsteren, A. DiNola and J. R. Haak, *J. Chem. Phys.*, 1984, **81**, 3648–3690.

48 B. Hess, H. Bekker, H. J. C. Berendsen and J. G. E. M. Fraaije, *J. Comput. Chem.*, 1997, **18**, 1463–1472.

49 T. Darden, D. York and L. Pedersen, *J. Chem. Phys.*, 1993, **98**, 10089–10092.

50 T. Darden, L. Perera, L. Li and L. Pedersen, *Structure*, 1999, R55–R60.

51 C. Blanchet, M. Pasi, K. Zakrzewska and R. Lavery, *Nucleic Acids Res.*, 2011, **39**(web server issue), W68–W73.

52 V. A. Bloomfield, D. M. Crothers, I. J. Tinoco, J. E. Hearst, D. E. Wemmer, P. A. Killman and D. H. Turner, *Nucleic Acids: Structures, Properties, and Functions*, University Science Books, Mill Valley, CA, 2000, pp. 88–91.

